Perovskite Solar Cells with 12.8% Efficiency by Using Conjugated Quinolizino Acridine Based Hole Transporting Material

ARTICLE *in* JOURNAL OF THE AMERICAN CHEMICAL SOCIETY · MAY 2014

Impact Factor: 12.11 · DOI: 10.1021/ja503272q · Source: PubMed

7 AUTHORS, INCLUDING:

Peng Qin
École Polytechnique Fédérale de Lausanne
18 PUBLICATIONS **1,566** CITATIONS
SEE PROFILE

Md Khaja Nazeeruddin
École Polytechnique Fédérale de Lausanne
489 PUBLICATIONS **44,964** CITATIONS
SEE PROFILE

JACS
JOURNAL OF THE AMERICAN CHEMICAL SOCIETY

Communication

pubs.acs.org/JACS

Perovskite Solar Cells with 12.8% Efficiency by Using Conjugated Quinolizino Acridine Based Hole Transporting Material

Peng Qin,[†] Sanghyun Paek,[‡] M. Ibrahim Dar,[†] Norman Pellet,[†] Jaejung Ko,[‡] Michael Grätzel,[†] and Mohammad Khaja Nazeeruddin*,[†]

[†]Laboratory of Photonics and Interfaces, Department of Chemistry and Chemical Engineering, Swiss Federal Institute of Technology, Station 6, CH-1015 Lausanne, Switzerland

[‡]Department of Advanced Materials Chemistry, Korea University, Jochiwon, Chungnam 339-700, Korea

Supporting Information

ABSTRACT: A low band gap quinolizino acridine based molecule was designed and synthesized as new hole transporting material in organic−inorganic hybrid lead halide perovskite solar cells. The functionalized quinolizino acridine compound showed an effective hole mobility in the same range of the state-of-the-art spiro-MeOTAD and an appropriate oxidation potential of 5.23 eV vs the vacuum level. The device based on this new hole transporting material achieved high power conversion efficiency of 12.8% under the illumination of 98.8 mW cm^{-2}, which was better than the well-known spiro-MeOTAD under the same conditions. Besides, this molecule could work alone without any additives, thus making it to be a promising candidate for solid-state photovoltaic application.

Organic−inorganic hybrid perovskite solar cells have emerged as attractive candidates for thin-film photovoltaic devices due to their high performance and low cost.[1−9] The $(RNH_3)PbX_3$ (R = alkyl, X = Cl, Br, I) are direct band gap materials and exhibit strong light harvesting ability across the visible solar spectrum. These materials are ambipolar and exhibit both electron and hole charge carrier mobility, making them potential candidates for solid-state photovoltaic devices.[10−16] Over the last two years, using perovskites as a light harvester and 2,2′,7,7′-tetrakis(*N*,*N*-dipmethoxyphenylamine)-9,9′-spirobifluorene (spiro-MeOTAD) as a hole transporting material (HTM), power conversion efficiencies (PCE) of over 15% were obtained.[17−19]

In the context of HTM, besides the state-of-the-art spiro-MeOTAD, the most efficient small molecule,[20] polymer,[21,22] and inorganic material[23,24] showed maximum efficiencies of 12.4%, 12.3%, and 12.4%, respectively. In all of these cases, the HTMs have almost no absorption in the visible and near-infrared (IR) regions. The colored low band gap donor−acceptor polymers with strong absorptions in this spectral region have also been tested as HTMs in perovskite solar cells, showing PCEs of 4.2−9.2%.[21,25,26] Similar to the colorless HTMs, the polymers only served as hole-transporter, whereas the perovskite act as the light harvester.

Here, we report on the synthesis, characterization, and photovoltaic application of a new low band gap small molecule HTM based on quinolizino acridine. The functionalized colored quinolizino acridine based compound works as an effective p-type HTM in $CH_3NH_3PbI_3$ solar cells, yielding power conversion efficiency of 12.8% under 98.8 mW cm^{-2} illumination.

The chemical structure of the molecularly engineered HTM is shown in Figure 1. The triarylamine core donor was flattened and functionalized with 4-[5-bromo-3,3′-dihexylsilylene-2,2′-bithio phene]-7-[5″-*n*-hexyl-(2,2′;5′,2″-terthiophene)-5-yl]-benzo[c]-[1,2, 5]thiadiazole groups to obtain a low band gap highly absorbing HTM. The flattened star-shaped organic hole conductor is expected to enhance the intermolecular $\pi-\pi$ packing interactions resulting efficient hole transport and increasing the lifetime of the charge-separated state. The benzothiadiazole unit was introduced for adjusting the HOMO and LUMO levels, and the corresponding experimental details are shown in the Supporting Information (SI).

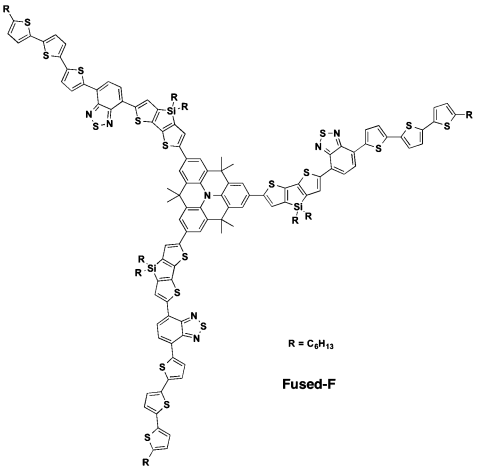

Figure 1. Molecular structure of the HTM Fused-F.

The UV−vis absorption and emission spectra of Fused-F in chloroform solution are shown in Figure 2a. In contrast to spiro-MeOTAD, which exhibits absorptions mainly in the UV region, Fused-F shows intensive charge-transfer absorption bands in the visible region with peaks at 421 nm (molar extinction coefficients ε = 108000 L mol^{-1} cm^{-1}) and 580 nm

Received: April 1, 2014

   dx.doi.org/10.1021/ja503272q | J. Am. Chem. Soc. XXXX, XXX, XXX−XXX

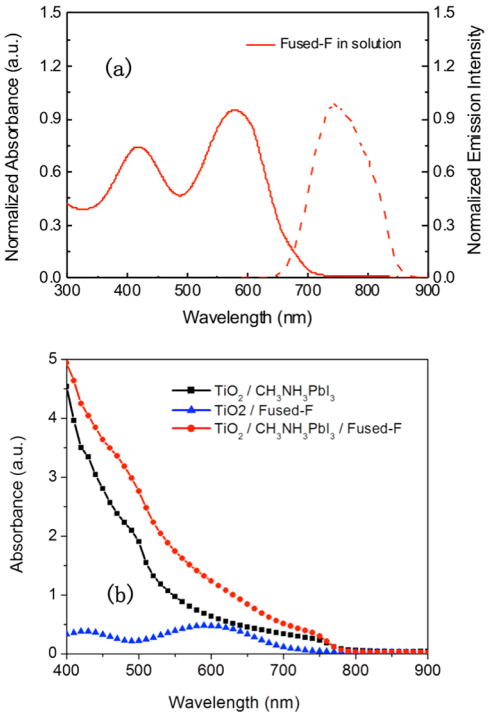

Figure 2. Optical characterization: (a) UV–vis absorption and fluorescence spectra of Fused-F in chloroform solution. (b) UV–vis absorption spectra of Fused-F coated on mesoporous TiO_2 and TiO_2/$CH_3NH_3PbI_3$ films. TiO_2/$CH_3NH_3PbI_3$ film without HTM is shown for comparison. Films used for the UV measurement are made under exactly the same conditions as the devices.

(ε = 135000 L mol^{-1} cm^{-1}). The visible light absorbing property of the Fused-F serves the purpose of harvesting the light, which is transmitted through the $CH_3NH_3PbI_3$ layer. The fluorescence spectrum shows a maximum emission at 746 nm, with a large Stokes shift of more than 150 nm. To further investigate the contribution of light absorption from Fused-F, the UV–vis spectra of $CH_3NH_3PbI_3$ films with and without Fused-F were recorded for comparison. As seen in Figure 2b, in the presence of Fused-F, a significant enhancement in absorption is observed in the whole visible region for the perovskite film, confirming the possibility of its additional contribution for light harvesting. We envisage that it harness the unabsorbed photons, which pass through the $CH_3NH_3PbI_3$ layer, therefore might contributing to the overall photocurrent generated by the device.

The thermal stability of Fused-F molecule was examined through thermal gravimetric analysis (TGA). The TGA shows that Fused-F is quite stable as it withstands very high temperatures and starts degrading only above 410 °C (Figure S1). The hole mobility of Fused-F was measured using charge extraction by linearly increasing voltage technique in the dark (Figure S2).[27,28] In the past this technique has been effectively used to characterize disordered organic semiconductors as it allows a straightforward determination of the majority charge carrier mobility.[29,30] We measured an effective hole mobility ranging from 3×10^{-5} to 6×10^{-5} cm^2 V^{-1} s^{-1} with electric fields ranging from 10^8 to 10^9 V cm^{-1}, which apparently falls in the same range to that of spiro-MeOTAD. To determine the highest occupied molecular orbital (HOMO) and the lowest unoccupied molecular orbital (LUMO) energy levels of Fused-F, we employed cyclic voltammetry (CV) (Figure S3). It was found that the Fused-F exhibits HOMO and LUMO levels at −5.23 and −3.66 eV, respectively. Under illumination, free charge carriers generated in the $CH_3NH_3PbI_3$ layer, could be extracted by transferring electron and holes, respectively, to TiO_2 and Fused-F as the energy levels are appropriate, thus the undesired recombination can be avoided.

Figure 3 shows the device architecture where fluorine-doped tin oxide glass substrate was first coated with a thin compact

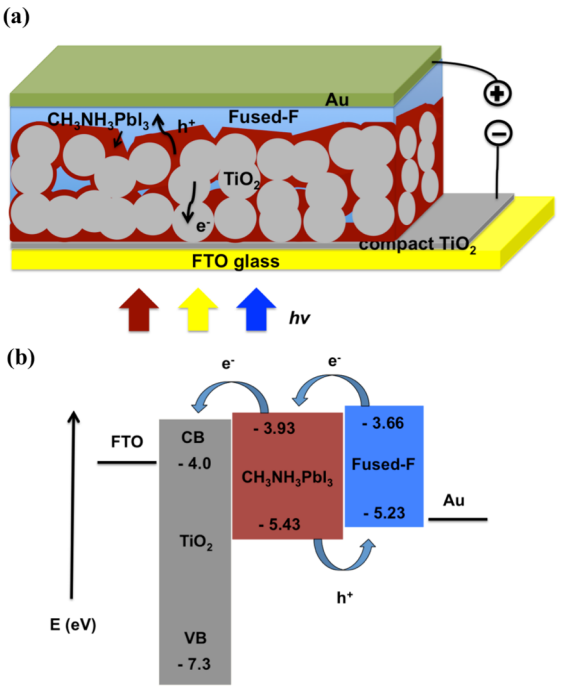

Figure 3. Device architecture and energy-level diagram: (a) Schematics of the whole device: FTO glass/compact TiO_2 layer/mesoporous TiO_2 with $CH_3NH_3PbI_3$/HTM/Au and the corresponding (b) energy level diagram.

TiO_2 as a hole blocking layer, followed by deposition of ∼250 nm mesoporous TiO_2 (m-TiO_2) layer which plays the role of scaffold as well as electron collector. Lead iodide (PbI_2) was deposited onto the mesoporous TiO_2 surface by spin-coating. After annealing, the PbI_2 film was immersed into a solution of methylammonium iodide (CH_3NH_3I) to form the perovskite $CH_3NH_3PbI_3$. The Fused-F HTM was then introduced by spin-coating from a chlorobenzene solution, and finally Au was evaporated as the back contact.

Surface morphology of TiO_2/$CH_3NH_3PbI_3$ films without and with HTM was examined using a high-resolution scanning electron microscope (SEM) as depicted in Figure 4. High-magnification SEM micrograph brings out the formation and uniform distribution of ∼100 nm $CH_3NH_3PbI_3$ nanocrystals over the surface of titanium dioxide photoanode (Figure 4a). With the presence of HTM, Figure 4b shows that the $CH_3NH_3PbI_3$ nanocrystals are uniformly covered with Fused-F. In addition to the infiltration into the mesoporous TiO_2, the $CH_3NH_3PbI_3$ forms an overlayer that is quite evident from the high-resolution cross-sectional SEM micrograph of the sample (Figure 4c). Similarly the Fused-F forms an overlayer besides infiltrating among the $CH_3NH_3PbI_3$ nanocrystals (Figure 4d).

The current–voltage (J–V) characteristics of $CH_3NH_3PbI_3$ based solar cell measured in dark and under simulated irradiation are shown in Figure 5a, and the corresponding

dx.doi.org/10.1021/ja503272q | J. Am. Chem. Soc. XXXX, XXX, XXX–XXX

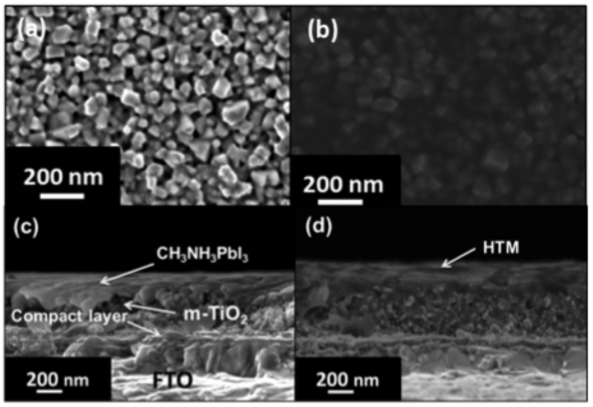

Figure 4. SEM characterization: High-magnification SEM micrographs of $CH_3NH_3PbI_3$ nanocrystals without (a) and with (b) Fused-F. Cross-sectional micrographs of $TiO_2/CH_3NH_3PbI_3$ (c) and $TiO_2/CH_3NH_3PbI_3$ /Fused-F (d).

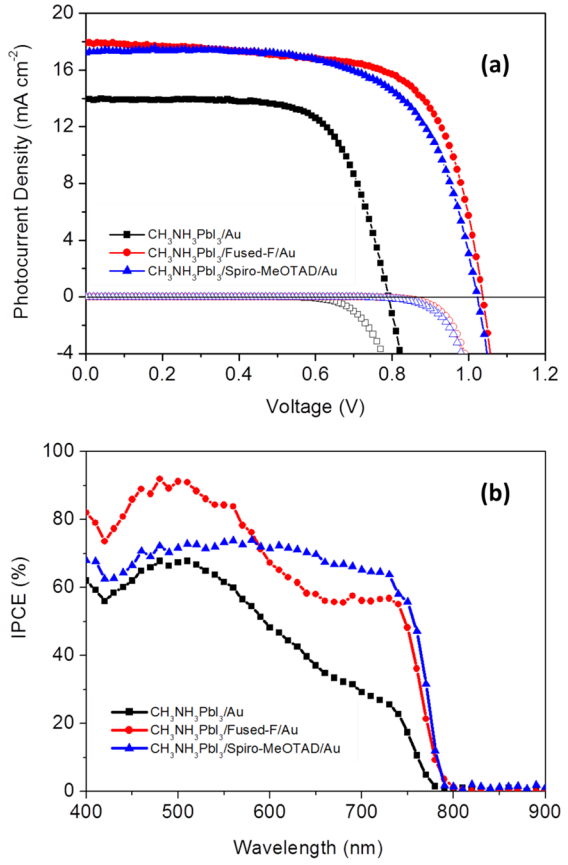

Figure 5. (a) Current−voltage characteristics of the solar cells with Fused-F (red), spiro-MeOTAD (blue) as the HTM, and without HTM (black) measured in the dark and under ∼100 mW cm^{-2} photon flux (AM 1.5G). (b) Corresponding IPCE spectra.

t1 photovoltaic parameters are summarized in Table 1. For comparative analysis, a reference cell without a HTM was fabricated. The best device with Fused-F shows a short-circuit current density (J_{sc}) of 17.9 mA/cm^2, an open-circuit voltage (V_{oc}) of 1036 mV, and a fill factor (FF) of 0.68, leading to a PCE of 12.8%. Statistical data on a batch of ten devices is shown in (Table S1), giving an average PCE of 11.6%. Under similar conditions, the device without HTM shows relatively lower J_{sc} and V_{oc}, yielding a PCE of 7.7%. Arguably, the high J_{sc}

Table 1. Photovoltaic Parameters Derived from *J*−*V* Measurements of $CH_3NH_3PbI_3$ Based Devices with Fused-F and spiro-MeOTAD as the HTM and without Any HTM for Comparison[a]

	light intensity (mW cm^{-2})	J_{sc} (mA cm^{-2})	V_{oc} (mV)	FF	PCE (%)
Fused-F	98.8	17.9	1036	0.68	12.8
spiro-MeOTAD	99.0	17.2	1022	0.66	11.7
no HTM	99.0	14.0	790	0.69	7.7

[a]Devices were masked with a black metal aperture to define the active area of 0.285 cm^2.

obtained from the device with Fused-F could be due to the effective charge extraction, as well as the improved light harvesting.

Comparing with the state-of-the-art HTM spiro-MeOTAD, Fused-F shows the hole mobility in the same range.[31] However, spiro-MeOTAD suffers from low conductivity in its pristine form and therefore requires a dopant and additives, such as lithium bis(trifluoromethyl sulfonyl)imide (LiTFSI) and 4-*tert*-butylpyridine (TBP), to make it more effective.[32] Whereas for Fused-F, none of these additives is necessary. The devices with spiro-MeOTAD were also made under similar conditions for comparison, showing J_{sc} of 17.2 mA/cm^2, V_{oc} of 1022 mV, FF of 0.66, and a final PCE of 11.7% under the optimized concentration (spiro-MeOTAD: 60 mM, Co dopant: 6 mM, TBP: 0.2 M, and LiTFSI: 0.03 M in chlorobenzene) (Figure 5). Without any additives and with low concentration of spiro-MeOTAD (30 mM spiro-MeOTAD in chlorobenzene), the PCE dramatically dropped to 5.7%, with J_{sc} of 14.8 mA/cm^2, V_{oc} of 812 mV and FF of 0.48. The overall PCE of such a device was even lower than the device without any HTM as the FF was lower, which can be attributed to a high series resistance or low conductivity.

To grasp deeper insight into the synergistic role played by Fused-F, the incident photo-to-current conversion efficiency (IPCE) spectra for the devices were recorded (Figure 5b). It was quite evident that the presence of both Fused-F (photoactive HTM) and spiro-MeOTAD (nonphotoactive HTM) enhanced the photocurrent in the whole visible region between 400 and 800 nm by improvising charge collection/extraction. The effective charge extraction decreases the carrier density within the bulk perovskite material which eventually brings down the rate of recombination.[33] The device with Fused-F showed much higher IPCEs in the blue region than that of a device with spiro-MeOTAD, indicating that the Fused-F could also contributes to the overall photocurrent besides acting as a hole transporting material.

In summary, we have designed molecularly a novel hole transporting material that exhibits suitable energy level and hole mobility to extract holes efficiently from perovskite. The Fused-F is a hybrid molecule that has both donor and acceptor functionalities to induce charge-transfer transitions within the molecule. With the presence of this HTM, open-circuit voltage of over 1 V and power conversion efficiency of 12.8% were obtained, which is considerably higher than the device without HTM which shows PCE of 7.7% only. Comparing with the state-of-the-art HTM spiro-MeOTAD, this material can be used alone without any additives and shows competitive photovoltaic performance. This novel and high-performing material offers a new design strategy toward developing more HTMs for photovoltaic applications.

dx.doi.org/10.1021/ja503272q | J. Am. Chem. Soc. XXXX, XXX, XXX−XXX

■ ASSOCIATED CONTENT

Supporting Information

Experimental details and additional figures. This material is available free of charge via the Internet at http://pubs.acs.org.

■ AUTHOR INFORMATION

Corresponding Author

mdkhaja.nazeeruddin@epfl.ch

Notes

The authors declare no competing financial interest.

■ ACKNOWLEDGMENTS

We acknowledge financial contribution from Greatcell Solar SA, Epalinges, Switzerland, the King Abdullah University of Science and Technology (KAUST, award no. KUS-C1-015-21), the European Community's Seventh Framework Programme "CE-Mesolight" EPFL ECR advanced grant agreement no. 247404. J.K. and M.K.N. thank the International Science and Business Belt Program through the Ministry of Education, Science and Technology (no. 2013K000496), and the Korean government (MEST)) program (no. 2013004800). M.K.N. thank the Center of Excellence for Advanced Materials Research (CEAMR), King Abdulaziz University, Jeddah, Saudi Arabia for Adjunct Professor position.

■ REFERENCES

(1) Kagan, C. R.; Mitzi, D. B.; Dimitrakopoulos, C. D. *Science* **1999**, *286*, 945.
(2) Kojima, A.; Teshima, K.; Shirai, Y.; Miyasaka, T. *J. Am. Chem. Soc.* **2009**, *131*, 6050.
(3) Im, J.-H.; Lee, C.-R.; Lee, J.-W.; Park, S.-W.; Park, N.-G. *Nanoscale* **2011**, *3*, 4088.
(4) Kim, H.-S.; Lee, C.-R.; Im, J.-H.; Lee, K.-B.; Moehl, T.; Marchioro, A.; Moon, S.-J.; Humphry-Baker, R.; Yum, J.-H.; Moser, J. E.; Grätzel, M.; Park, N.-G. *Sci. Rep.* **2012**, *2*, 591:1.
(5) Lee, M. M.; Teuscher, J.; Miyasaka, T.; Murakami, T. N.; Snaith, H. J. *Science* **2012**, *338*, 643.
(6) Ball, J. M.; Lee, M. M.; Hey, A.; Snaith, H. J. *Energy Environ. Sci.* **2013**, *6*, 1739.
(7) Conings, B.; Baeten, L.; Dobbelaere, C. D.; ÒHaen, J.; Manca, J.; Boyen, H.-G. *Adv. Mater.* **2014**, *26*, 2041.
(8) Eperon, G. E.; Burlakov, V. M.; goriely, A.; Snaith, H. J. *ACS Nano* **2014**, *8*, 591.
(9) Chen, Q.; Zhou, H.; Hong, Z.; Luo, S.; Duan, H.-S.; Wang, H.-H.; Liu, Y.; Li, G.; Yang, Y. *J. Am. Chem. Soc.* **2014**, *136*, 622.
(10) Etgar, L.; Gao, P.; Xue, Z.; Qin, P.; Chandiran, A. K.; Liu, B.; Nazeeruddin, M. K.; Grätzel, M. *J. Am. Chem. Soc.* **2012**, *134*, 17396.
(11) Abrusci, A.; Stranks, S. D.; Docampo, P.; Yip, H.-L.; Jen, L. K-Y.; Snaith, H. J. *Nano Lett.* **2013**, *13*, 3124.
(12) Qin, P.; Domanski, A. L.; Chandiran, A. K.; Berger, R.; Butt, H.-J.; Dar, M. I.; Moehl, T.; Tetreault, N.; Gao, P.; Ahmad, S.; Nazeeruddin, M. K.; Grätzel, M. *Nanoscale* **2014**, *6*, 1508.
(13) Malinkiewicz, O.; Yella, A.; Lee, Y.-H.; Espallargas, G. M.; Grätzel, M.; Nazeeruddin, M. K.; Bolink, H. J. *Nat. Photonics* **2014**, *8*, 128.
(14) Stranks, S. D.; Eperon, G. E.; Grancini, G.; Menelaou, C.; Alcocer, M. J. P.; Leijtens, T.; Herz, L. M.; Petrozza, A.; Snaith, H. J. *Science* **2013**, *342*, 341.
(15) Xing, G.; Mathews, N.; Sun, S.; Lim, S. S.; Lam, Y. M.; Grätzel, M.; Mhaisalkar, S.; Sum, T. C. *Science* **2013**, *342*, 344.
(16) Kim, H.-S.; Mora-Sero, I.; Gonzalez-Pedro, V.; Fabregat-Santiago, F.; Juarez-Perez, E. J.; Park, N.-G.; Bisquert, J. *Nat. Commun.* **2013**, *4*, 2242:1.
(17) Burschka, J.; Pellet, N.; Moon, S.-J.; Humphry-Baker, R.; Gao, P.; Nazeeruddin; Grätzel, M. *Nature* **2013**, *499*, 316.
(18) Liu, M.; Johnston, M. B.; Snaith, H. J. *Nature* **2013**, *501*, 395.
(19) Liu, D.; Kelly, T. L. *Nat. Photonics* **2014**, *8*, 133.
(20) Jeon, N. J.; Lee, J.; Noh, J. H.; Nazeeruddin, M. K.; Grätzel, M.; Seok, S. I. *J. Am. Chem. Soc.* **2013**, *135*, 19087.
(21) Heo, J. H.; Im, S. H.; Noh, J. H.; Mandal, T. N.; Lim, C.-S.; Chang, J. A.; Lee, Y. H.; Kim, H.-J.; Sarkar, A.; Nazeeruddin, M. K.; Grätzel, M.; Seok, S. I. *Nat. Photonics* **2013**, *7*, 486.
(22) Noh, J. H.; Im, S. H.; Heo, J. H.; Mandal, T. N.; Seok, S. I. *Nano Lett.* **2013**, *13*, 1764.
(23) Christians, J. A.; Fung, R. C. M.; Kamat, P. V. *J. Am. Chem. Soc.* **2014**, *136*, 758.
(24) Qin, P.; Tanaka, S.; Ito, S.; Tetreault, N.; Manabe, K.; Nishino, H.; Nazeeruddin, M. K.; Grätzel, M. *Nat. Commun.* **2014**, DOI: 10.1038/ncomms4834.
(25) Cai, B.; Xing, Y.; Yang, Z.; Zhang, H.-W.; Qiu, J. *Energy Environ. Sci.* **2013**, *6*, 1480.
(26) Kwon, Y. S.; Lim, J.; Yun, H.-J.; Kim, Y.-H.; Park, T. *Energy Environ. Sci.* **2014**, *7*, 1454.
(27) Lorrmann, J.; Badada, B. H.; Inganäs, O.; Dyakonov, V.; Deibel, C. *J. Appl. Phys.* **2010**, *108*, 113705.
(28) Mozer, A. J.; Sariciftci, N. S.; Lutsen, L.; Vanderzande, D.; Österbacka, R.; Westerling, M.; Juška, G. *Appl. Phys. Lett.* **2005**, *86*, 112104.
(29) Juška, G.; Arlauskas, K.; Viliūnas, M. *Phys. Rev. Lett.* **2000**, *84*, 4946.
(30) Österbacka, R.; Pivrikas, A.; Juška, G.; Genevičius, K.; Arlauskas, K.; Stubb, H. *Curr. Appl. Phys.* **2004**, *4*, 534.
(31) Leijtens, T.; Ding, I.-K.; Giovenzana, T.; Bloking, J. T.; McGehee, M. D.; Sellinger, A. *ACS Nano* **2012**, *6*, 1455.
(32) Burschka, J.; Dualeh, A.; Kessler, F.; Baranoff, E.; Cevey-Ha, N.-L.; Yi, C.; Nazeeruddin, M. K.; Grätzel, M. *J. Am. Chem. Soc.* **2011**, *133*, 18042.
(33) Juarez-Perez, E.; Wuβler, M.; Fabregat-Santiago, F.; Lakus-Wollny, K.; Mankel, E.; Mayer, T.; Jaegermann, W.; Mora-Sero, I. *J. Phys. Chem. Lett.* **2014**, *5*, 680.